

## Effect of surface structure on crystal-truncation-rod scattering under the Bragg condition

T. Takahashi,\* W. Yashiro, M. Takahashi,<sup>†</sup> and S. Kusano

*Institute for Solid State Physics, The University of Tokyo, Kashiwanoha, Kashiwa, Chiba 277-8581, Japan*

X. W. Zhang and M. Ando

*Institute of Materials Structure Science, High Energy Accelerator Research Organization, Oho, Tsukuba, Ibaraki 305-0801, Japan*

(Received 19 July 1999; revised manuscript received 8 February 2000)

Theoretical and experimental studies have been made on crystal-truncation-rod (CTR) scattering when x rays satisfy the Bragg condition. Calculations were made on the basis of a dynamical theory in Darwin's approach extended to a multibeam case. Calculated results indicated that the profile of intensity changes of CTR scattering as a function of incident angle under the Bragg condition is sensitive to surface structures. It was made clear by kinematical treatment that the profile reflects x-ray intensity changes of the standing-wave field at an atomic layer on a substrate crystal when x-ray scattering amplitude by the surface layer is larger than CTR scattering amplitude by the substrate, particularly in the case of intensity measurements on fractional-order rods of superstructures formed on the substrate crystal. The experimental result obtained for a Si (001) crystal was in good agreement with the theoretical calculation. Detailed analysis suggested that a strain field caused by the native oxide layer spreads from the surface of the substrate crystal to a depth of hundreds of Å.

### I. INTRODUCTION

X-ray diffraction has been used to study the structure of surfaces and interfaces in recent decades.<sup>1,2</sup> Grazing incidence diffraction is very powerful in determining two-dimensional structures projected on surfaces.<sup>3</sup> On the other hand, crystal-truncation-rod (CTR) scattering has been successfully used to determine three-dimensional structures of surfaces including superstructures formed on substrates.<sup>4-9</sup> One of the advantages of using x-ray scattering in surface structure analysis is that the scattering process is explained by the kinematical theory of single scattering while multiple scattering processes are to be taken into account in electron diffraction such as low-energy electron diffraction and reflection high-energy electron diffraction.

As in the case of electron diffraction, x rays incident on a plate crystal are diffracted in all the directions determined by the intersections between the Ewald sphere and the reciprocal rods. Therefore, in principle one can observe those diffraction spots simultaneously. Even in that case, however, those intensities are analyzed independently in x-ray diffraction because the intensity of CTR scattering is extremely weak compared with that of Bragg reflection. It should be noted, however, that this assumption is correct only when no Bragg scattering is excited by the crystal. When the Bragg condition is satisfied for at least one Bragg point, all the intensities of CTR scattering are expected to be influenced by the Bragg reflected beam.

In this work, we study an influence of Bragg reflection on CTR scattering. We show that the intensity of CTR scattering changes drastically as a function of incidence angle under the Bragg condition, and the profile of the intensity change is sensitive to surface structures using a dynamical theory developed by us.<sup>10</sup> Reasons for surface sensitivities of the profile are discussed in comparison with the x-ray standing wave (XSW) method<sup>11</sup> by using the kinematical approxi-

mation for interaction between Bragg scattering and CTR scattering. Finally an experimental result is given using a Si (001) crystal.

### II. DYNAMICAL TREATMENT BY DARWIN THEORY EXTENDED TO MULTIBEAM CASE

The intensity of CTR scattering has been well understood based on the kinematical theory.<sup>1,4</sup> Recently, CTR scattering has been studied from viewpoints of dynamical diffraction,<sup>10,12-17</sup> and the intensity profile of CTR scattering along rods is interpreted as a tail of the rocking curve in dynamical diffraction phenomena. This means that the rocking angle, that is, the deviation parameter such as  $\eta$ ,<sup>11</sup> can be related to the perpendicular momentum transfer indexed by  $l$ . In a previous work, we generalized the deviation parameter so that it can be applied to any angles not only around the Bragg angle but also far from the Bragg angle.<sup>10,18</sup>

To study an influence of Bragg reflection on CTR scattering, one is required to apply the dynamical theory to a multibeam case. A number of studies have been made on multibeam cases when only Bragg reflections are excited.<sup>19,20</sup> In contrast to this, there has been few works on a multibeam case where CTR scattering as well as Bragg reflection is taken into account.<sup>10,21</sup> This is because in the conventional dynamical theory, one can obtain diffracted intensities only when tie points very close to Bragg points are excited.

#### A. Theoretical

In this work, we study CTR scattering under the Bragg condition based on a dynamical theory<sup>10</sup> in Darwin's approach.<sup>22</sup> Features of the theory are that not only can it calculate the intensity of CTR scattering far from Bragg points as well as near Bragg points, but also it can be easily extended to the case where the crystal is covered with surface layers.

In this work, we treat a three-beam case, but it does not lose generality because the interaction between CTR scatterings is much weaker than that between Bragg scattering and CTR scattering. For simplicity, we treat a coplanar Bragg case where the incident and two reflected beams are in a plane perpendicular to the crystal surface.

First, we consider the case of a perfect crystal of semi-infinite thickness. Figure 1(a) illustrates a diffraction condition where a Bragg point  $H_1$  on the  $h_1k_1$  rod and a point  $H_2$  on the  $h_2k_2$  rod are excited. Reflection coefficients of two diffracted beams  $R_{H_1}^B$  and  $R_{H_2}^B$  by a perfect crystal of semi-

infinite thickness in the coplanar case are given in Ref. 10 and are summarized in the Appendix with some details. The expressions giving  $R_{H_1}^B$  and  $R_{H_2}^B$  are valid for any incidence angle provided the Ewald sphere intersects with the two rods in reflection geometry.

Once the reflection coefficients from an ideally truncated perfect crystal are obtained for the two beams  $H_1$  and  $H_2$ , those from the crystal whose surface is covered by a surface layer,  $R_{H_1}$  and  $R_{H_2}$ , are given as follows by considering multiple-scattering processes between the surface layer and the perfect crystal of semi-infinite thickness,

$$R_{H_1} = \frac{r_{H_1}^s + (t_0^s t_{H_1}^s - r_{H_1}^s r_{H_1}^s) \Phi_0^s \Phi_{H_1}^s R_{H_1}^B + (t_0^s r_{H_1-H_2}^s - r_{H_1}^s r_{H_2}^s) \Phi_0^s \Phi_{H_2}^s R_{H_2}^B}{1 - (r_{H_1}^s \Phi_0^s \Phi_{H_1}^s R_{H_1}^B + r_{H_2}^s \Phi_0^s \Phi_{H_2}^s R_{H_2}^B)}, \quad (1)$$

$$R_{H_2} = \frac{r_{H_2}^s + (t_0^s r_{H_2-H_1}^s - r_{H_1}^s r_{H_2}^s) \Phi_0^s \Phi_{H_1}^s R_{H_1}^B + (t_0^s t_{H_2}^s - r_{H_2}^s r_{H_2}^s) \Phi_0^s \Phi_{H_2}^s R_{H_2}^B}{1 - (r_{H_1}^s \Phi_0^s \Phi_{H_1}^s R_{H_1}^B + r_{H_2}^s \Phi_0^s \Phi_{H_2}^s R_{H_2}^B)}. \quad (2)$$

Here we assumed the surface structure has two-dimensional periodicity commensurate with the substrate crystal. In these equations  $t^s$ 's and  $r^s$ 's are transmission and reflection coefficients of x rays by the surface layer, respectively, which are calculated by Fresnel's diffraction theory taking into account single scattering.<sup>10,23</sup> The surface layer does not necessarily mean a single atomic plane. A small number of atomic planes are allowed if the effect of multiple scattering among the planes is neglected. Phase factors  $\Phi_0^s$ ,  $\Phi_{H_1}^s$ , and  $\Phi_{H_2}^s$  correspond to phase changes due to traveling paths between the surface layer and the substrate, and thus are related to the thickness  $d^s$  of the surface layer and the propagating directions of the three beams as is seen in Eqs. (A4) of the Appendix.

## B. Simulations

To investigate an influence of Bragg reflection on CTR scattering, we simulated intensities of CTR scattering along the 50 rod of an ideally truncated perfect Si crystal with (001) surface under excitation of 004 Bragg reflection on the 00 rod, as shown in Fig. 2. By changing the wavelength, we can select the index  $l$  on the 50 rod while exciting the 004 Bragg point on the 00 rod.

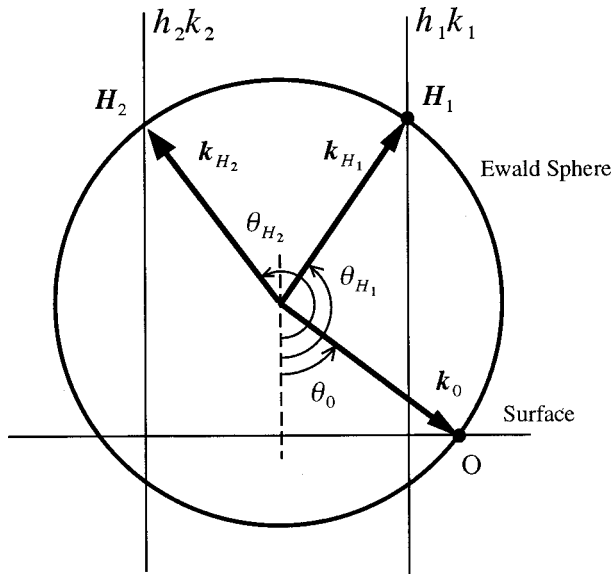
First, we show results when the topmost surface layer is displaced only in the direction of surface normal, corresponding to the direction of the scattering vector for the 004 Bragg point. Here we displaced, for simplicity, the topmost 001 layer, which is a set of four atomic planes corresponding to the unit cell in the ordinal definition.

Figures 3(a), 3(b), and 3(c) show intensity changes calculated for the 50 rod around  $l=5.013$ ,  $l=4.924$ , and  $l=4.423$ , respectively. Here the index  $l$  was defined so that  $l=4$  means the 004 Bragg point. Then  $l=5$  corresponds to the kinematical 555 Bragg reflection. To excite these points designated by  $l$  values on the 50 rod while satisfying the 004

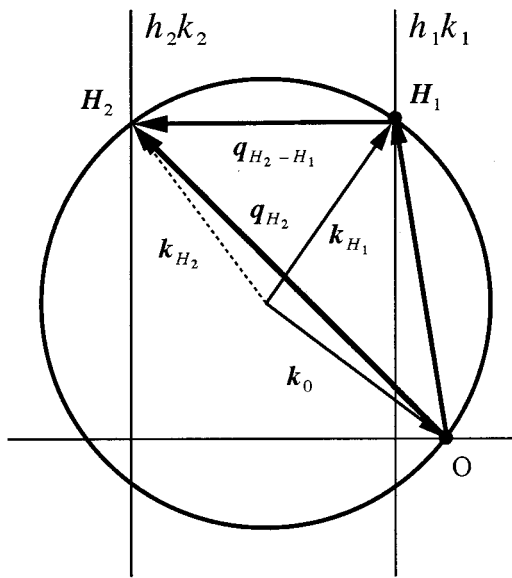
Bragg condition, the wavelengths of  $\lambda=1.24053 \text{ \AA}$ ,  $1.25000 \text{ \AA}$ , and  $1.30000 \text{ \AA}$  were used in the simulations. Percent values shown in the insets of the figures mean the displacement of the topmost layer normal to the surface, and the value of 100% corresponds to the displacement equivalent to the distance between (004) atomic planes,  $5.4310/4 \text{ \AA}$ .

In the condition of Fig. 3(a), where a point very close to the Bragg point is excited, the profile shows little change with the displacement of the surface layer, being insensitive to the surface structure as is expected. However, as the excited point goes farther from the Bragg point, the intensity profile of CTR scattering becomes sensitive to the displacement of the surface layer as seen in Figs. 3(b) and 3(c). The profile of intensity changes in Fig. 3(c) depends strongly on the displacement of the surface layer, and resembles that of secondary emission in XSW,<sup>11</sup> the reason of which is discussed in the next section based on the kinematical approximation.

Next, we show effects of the displacement of the surface layer on the intensity of CTR scattering when the displacement has a component parallel to the surface. We made simulations for the case of Fig. 3(c) ( $\lambda=1.30000 \text{ \AA}$ ) where the profile is most sensitive to the change of the surface structure. Figures 4(a), 4(b), 4(c), and 4(d) show results calculated for the displacement in the direction of  $\mathbf{a}_1^s$ , where  $\mathbf{a}_1^s$  was defined by  $\mathbf{a}_1^s = \frac{1}{2}\mathbf{a}_1 + \frac{1}{2}\mathbf{a}_2$  in the (001) surface of silicon. In the figures, the displacement of the surface layer in the direction of surface normal was fixed at 0%, 25%, 50%, and 75% of  $\mathbf{a}_3/4$ , respectively, corresponding to Fig. 3(c). Percent values shown in the insets represent the ratio of the displacement in the direction of  $\mathbf{a}_1^s$  to that corresponding to  $|\mathbf{a}_1^s|/5$ , that is,  $5.4310/(5\sqrt{2})\text{ \AA}$ . One should note that the intensity profile of 100% displacement is identical to that of no displacement, which comes from the fact that the present simulation is done along the 50 rod.



(a)



(b)

FIG. 1. Geometry of coplanar three-beam case (a) and relations among wave vectors used to explain the effect of Bragg scattering on CTR scattering (b).

### III. QUALITATIVE INTERPRETATION BY KINEMATICAL THEORY

In this section, we show how the intensity of CTR scattering is modulated by Bragg reflection on the basis of the kinematical approximation, comparing with the intensity change of secondary emission in XSW. We use the dynamical theory only for Bragg reflection and utilize the phase relationship between the incident and diffracted waves. As for other interactions, kinematical approximations are used.

#### A. Standing-wave field under Bragg condition

First, we briefly review XSW in the two-beam case.<sup>11</sup> When x rays are incident on an ideal crystal of semi-infinite thickness at an angle satisfying the Bragg condition with

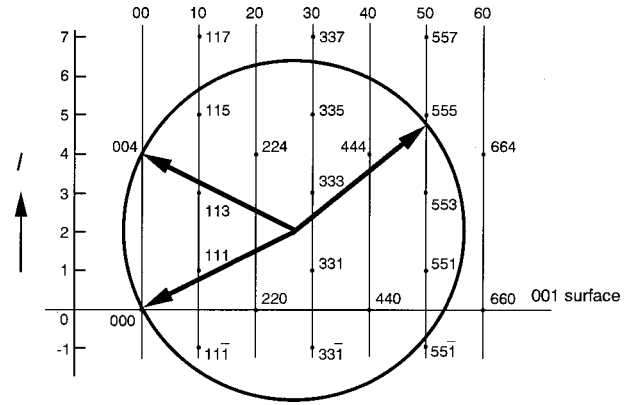


FIG. 2. Geometry used in the simulation.

respect to a reciprocal point  $\mathbf{H}$ , then a standing wave field is generated in the crystal as a result of interference between the incident and diffracted waves. The electric field at a point  $\mathbf{r}$  in the crystal is given by

$$\mathbf{E} = \mathbf{E}_0 \exp(-2\pi i \mathbf{k}_0 \cdot \mathbf{r}) + \mathbf{E}_H \exp(-2\pi i \mathbf{k}_H \cdot \mathbf{r}). \quad (3)$$

Here  $\mathbf{k}_0$  and  $\mathbf{k}_H$  are the wave vectors of the incident and diffracted waves in the crystal, respectively, and  $E_0$  and  $E_H$  are their amplitudes at  $\mathbf{r} = \mathbf{0}$ . From the dynamical theory of x-ray diffraction, the reflection coefficient for the semi-infinite crystal,  $R = E_H/E_0$ , is written in a well-known form as a function of deviation parameter  $\eta$  representing the incidence condition:

$$R = -|b|^{1/2} \frac{C}{|C|} \frac{F_H}{[F_H F_{\bar{H}}]^{1/2}} [\eta \pm (\eta^2 - 1)^{1/2}], \quad (4)$$

where  $C$  is the polarization factor,  $b$  is the asymmetric factor, and  $F_H$  is the structure factor for  $H$  reflection.

For the moment, we neglect absorption by the crystal to interpret phenomena qualitatively. Then the imaginary part of the deviation parameter  $\eta$  is neglected. In the region of total reflection  $-1 \leq \eta \leq 1$ , Eq. (4) can be rewritten by

$$R = -|b|^{1/2} \frac{C}{|C|} \frac{F_H}{[F_H F_{\bar{H}}]^{1/2}} [\eta - i(1 - \eta^2)^{1/2}] \quad (5)$$

$$= -|b|^{1/2} \frac{C}{|C|} \frac{F_H}{[F_H F_{\bar{H}}]^{1/2}} e^{-i\Pi(\eta)} \quad (6)$$

$$= |b|^{1/2} \sigma e^{-i\Pi(\eta)}, \quad (7)$$

where

$$\Pi(\eta) \equiv \tan^{-1} \left( \frac{\sqrt{1 - \eta^2}}{\eta} \right), \quad (8)$$

$$\sigma \equiv - \frac{C}{|C|} \frac{F_H}{[F_H F_{\bar{H}}]^{1/2}}. \quad (9)$$

From Eq. (7), the electric field given by Eq. (3) can be rewritten as follows:

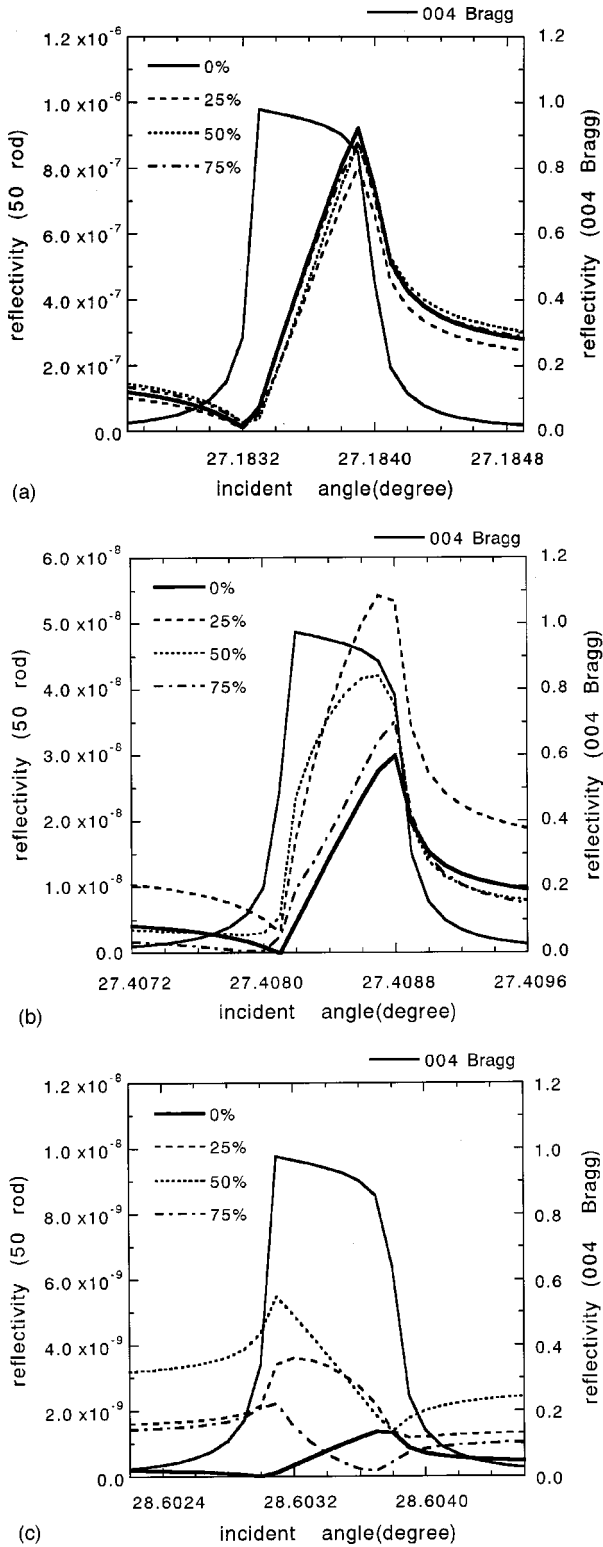


FIG. 3. Intensity changes of CTR scattering of 50 rod when 004 Bragg reflection is excited. Values of  $l$  when 004 Bragg point is excited are 5.0126 (a), 4.9237 (b) and 4.4231 (c).

$$\mathbf{E} = E_0 \exp(-2\pi i \mathbf{k}_0 \cdot \mathbf{r}) \{ \hat{\mathbf{E}}_0 + \hat{\mathbf{E}}_H |b|^{1/2} \sigma \exp[-i\Pi(\eta)] \times \exp[-2\pi i \mathbf{H} \cdot \mathbf{r}] \}, \quad (10)$$

using unit vectors,  $\hat{\mathbf{E}}_0$  and  $\hat{\mathbf{E}}_H$ . Therefore, the wave-field intensity at a point  $\mathbf{r}$  near the surface  $I$  is obtained as

$$I = |E_0|^2 \{ 1 + |b| + 2|b|^{1/2} \sigma C \cos[2\pi \mathbf{H} \cdot \mathbf{r} + \Pi(\eta)] \} \quad (11)$$

forming the standing wave. The antinodes of the standing wave are planes parallel to and have the same periodicity as the diffraction planes, and move from the middle of the diffraction planes to the position just on them with a change in  $\eta$  from 1 to  $-1$ , where  $\eta=1$  corresponds to the shoulder of the Darwin curve on the lower incident angle side.

### B. CTR scattering under excitation of Bragg reflection

Since the intensity of CTR scattering is sufficiently weak compared with that of Bragg reflection, one can treat CTR scattering by the kinematical theory. Now, we obtain the CTR scattering intensity based on the kinematical theory when Bragg reflection is excited on one of the rods. The CTR scattering field, whose direction is defined by wave vector  $\mathbf{k}_{H_2}$ , is composed of two components: one is generated from the incident wave  $\mathbf{k}_0$ , and the other from the diffracted wave  $\mathbf{k}_{H_1}$ . The scattering vector  $\mathbf{q}$  of each scattering process is given by

$$\mathbf{q}_{H_2} = \mathbf{k}_{H_2} - \mathbf{k}_0 \quad (12)$$

$$= h_{H_2} \mathbf{a}_1^* + k_{H_2} \mathbf{a}_2^* + l_{H_2} \mathbf{a}_3^* \quad (13)$$

and

$$\mathbf{q}_{H_2-H_1} = \mathbf{k}_{H_2} - \mathbf{k}_{H_1} \quad (14)$$

$$= h_{H_2-H_1} \mathbf{a}_1^* + k_{H_2-H_1} \mathbf{a}_2^* + l_{H_2-H_1} \mathbf{a}_3^*, \quad (15)$$

using the reciprocal vectors  $\mathbf{a}_i^*$  ( $i=1, 2, \text{ and } 3$ ).

According to the kinematical theory, the amplitude of CTR scattering by a perfect crystal of semi-infinite thickness is given by

$$F(\mathbf{q}) = F_{hk}(l) \sum_{N=0}^{-\infty} \exp(2\pi i N l) \\ = \frac{F_{hk}(l)}{1 - \exp(-2\pi i l)} = F_{hk}(l) \frac{\exp(\pi i l)}{2i \sin(\pi l)} \quad (16)$$

with respect to the scattering vector  $\mathbf{q} = h\mathbf{a}_1^* + k\mathbf{a}_2^* + l\mathbf{a}_3^*$ . Therefore, the amplitude of CTR scattering under the Bragg condition can be written in the following form:

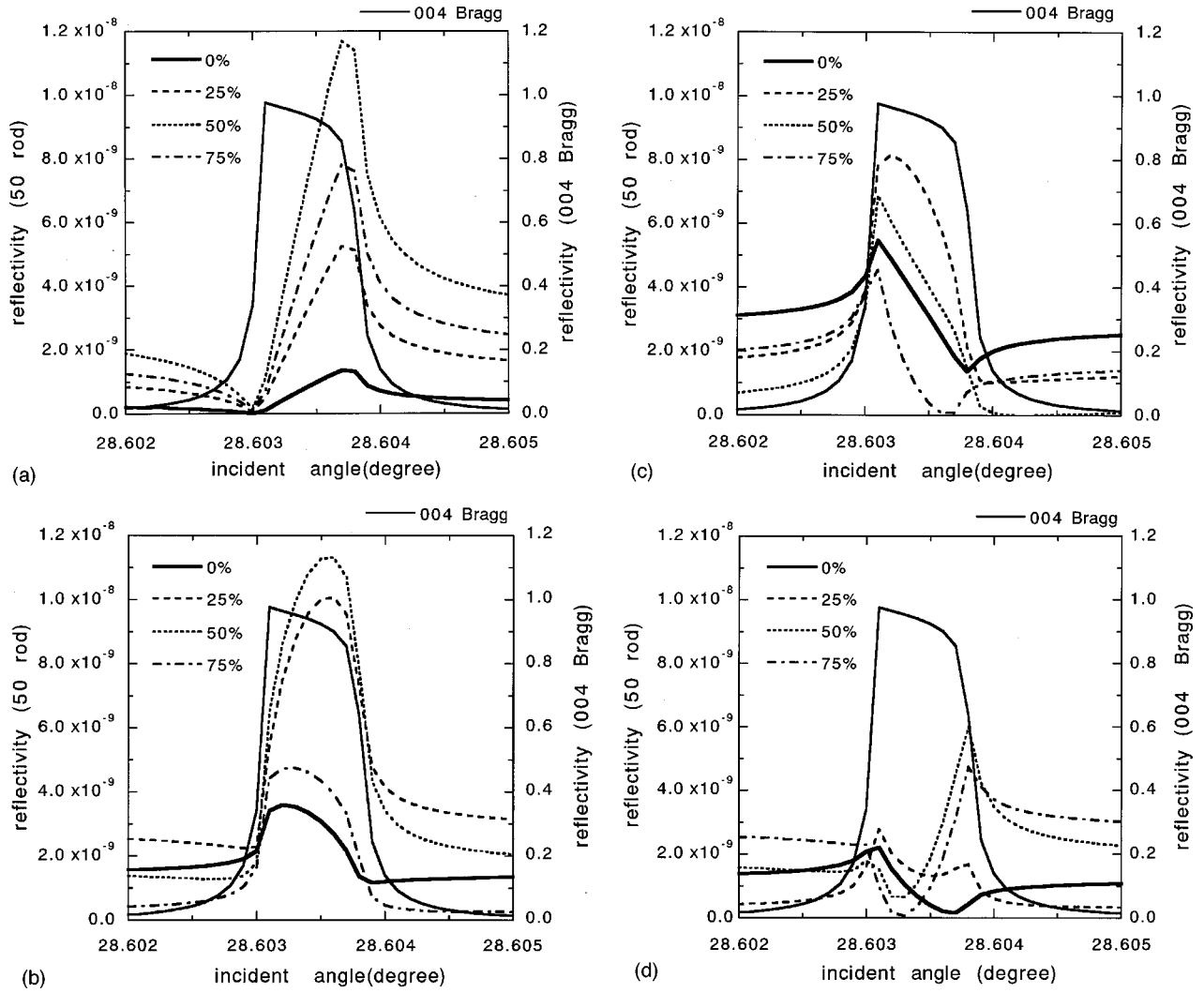


FIG. 4. Intensity changes of CTR scattering of 50 rod when 004 Bragg reflection is excited. Displacement in the direction to the surface normal is fixed to 0% (a), 25% (b), 50% (c), and 75% (d) of the distance between the (004) planes.

$$A^{\text{CTR}}(\mathbf{k}_{H_2}) \propto C_{H_2} F_{h_{H_2} k_{H_2}}(l_{H_2}) \frac{\exp(\pi i l_{H_2})}{2i \sin(\pi l_{H_2})} + C_{H_2-H_1} |b|^{1/2} \sigma F_{h_{H_2-H_1} k_{H_2-H_1}}(l_{H_2-H_1}) \frac{\exp(\pi i l_{H_2-H_1})}{2i \sin(\pi l_{H_2-H_1})} \exp[-i\Pi(\eta)], \quad (17)$$

using Eq. (10). Here,  $C_{H_2}$  and  $C_{H_2-H_1}$  are the polarization factors associated with  $\mathbf{q}_{H_2}$  and  $\mathbf{q}_{H_2-H_1}$ , respectively.

The scattering vectors  $\mathbf{q}_{H_2}$  and  $\mathbf{q}_{H_2-H_1}$  are not independent, having a relation of

$$\mathbf{q}_{H_2-H_1} - \mathbf{q}_{H_2} = -(\mathbf{k}_{H_1} - \mathbf{k}_0) = -\mathbf{H}_1, \quad (18)$$

as shown in Fig. 1(b). Then, we obtain a relation of

$$l_{H_2-H_1} - l_{H_2} = -l_{H_1}. \quad (19)$$

Since  $l_{H_1}$  takes an integer when the Bragg condition is satisfied, Eq. (17) is rewritten by

$$A^{\text{CTR}}(\mathbf{k}_{H_2}) \propto \frac{\exp(\pi i l_{H_2})}{2i \sin(\pi l_{H_2})} \{ C_{H_2} F_{h_{H_2} k_{H_2}}(l_{H_2}) + C_{H_2-H_1} |b|^{1/2} \sigma F_{h_{H_2-H_1} k_{H_2-H_1}}(l_{H_2-H_1}) \} \times \exp[-i\Pi(\eta)]. \quad (20)$$

Therefore the intensity is given as follows:

$$I^{\text{CTR}}(\mathbf{k}_{H_2}) \propto \frac{1}{4 \sin^2(\pi l_{H_2})} | C_{H_2} F_{h_{H_2} k_{H_2}}(l_{H_2}) + C_{H_2-H_1} |b|^{1/2} \sigma F_{h_{H_2-H_1} k_{H_2-H_1}}(l_{H_2-H_1}) \times \exp[-i\Pi(\eta)] |^2. \quad (21)$$

In the case of a centrosymmetric crystal, the imaginary parts of the structure factors  $F$ 's are zero by a proper selection of the origin for the unit cell. Then in the case of an ideal crystal, we notice the intensity change of CTR scattering as a function of  $\eta$  is similar to that of the standing wave field at  $\mathbf{r}=0$  from Eq. (11) when the condition of

$$C_{H_2} F_{h_{H_2} k_{H_2}}(l_{H_2}) C_{H_2-H_1} F_{h_{H_2-H_1} k_{H_2-H_1}}(l_{H_2-H_1}) > 0 \quad (22)$$

is satisfied for the diffraction condition, which is the case in the simulations given in the previous section. This explains why the intensity change in the case of no displacement 0% in Figs. 3(a), 3(b), and 3(c) is insensitive to the point of  $l$ , showing similar profiles as the intensity change of the standing wave field at the diffracting planes.

When the surface of the crystal is not ideally truncated, the effect of the surface structure on x-ray scattering has to be taken into account. Then the electric-field amplitude is rewritten by

$$\begin{aligned} A^{\text{CTR}} \propto & C_{H_2} \left[ F_{h_{H_2} k_{H_2}}(l_{H_2}) \frac{\exp(\pi i l_{H_2})}{2i \sin(\pi l_{H_2})} \right. \\ & \left. + F_{h_{H_2} k_{H_2}}^s(l_{H_2}) \exp(2\pi i \mathbf{q}_{H_2} \cdot \mathbf{r}^s) \right] \\ & + C_{H_2-H_1} |b|^{1/2} \sigma \left[ F_{h_{H_2-H_1} k_{H_2-H_1}}(l_{H_2-H_1}) \right. \\ & \times \frac{\exp(\pi i l_{H_2-H_1})}{2i \sin(\pi l_{H_2-H_1})} \\ & \left. + F_{h_{H_2-H_1} k_{H_2-H_1}}^s(l_{H_2-H_1}) \exp(2\pi i \mathbf{q}_{H_2-H_1} \cdot \mathbf{r}^s) \right] \\ & \times \exp[-i\Pi(\eta)], \quad (23) \end{aligned}$$

where  $\mathbf{r}^s$  is the position of the surface structure relative to the substrate, and  $F_{hk}^s$  is the structure factor for the surface structure.

Using this equation, we can almost reproduce the results in the previous section calculated by the dynamical theory. This equation clearly shows that the total scattering amplitude at far from the Bragg point is sensitive to the structure of the surface layer. In an extreme case where the amplitude from the substrate is neglected compared with that from the surface layer, the total amplitude is given by

$$\begin{aligned} A^{\text{CTR}} \propto & \exp(2\pi i \mathbf{q}_{H_2} \cdot \mathbf{r}^s) \{ C_{H_2} F_{h_{H_2} k_{H_2}}^s(l_{H_2}) \\ & + C_{H_2-H_1} |b|^{1/2} \sigma F_{h_{H_2-H_1} k_{H_2-H_1}}^s(l_{H_2-H_1}) \\ & \times \exp(-2\pi i \mathbf{H}_1 \cdot \mathbf{r}^s) \exp[-i\Pi(\eta)] \}. \quad (24) \end{aligned}$$

This means that the dependence of the intensity modulation of CTR scattering on the position of the surface layer relative to the substrate crystal is similar to that of secondary emission in XSW, as seen from Eq. (10).

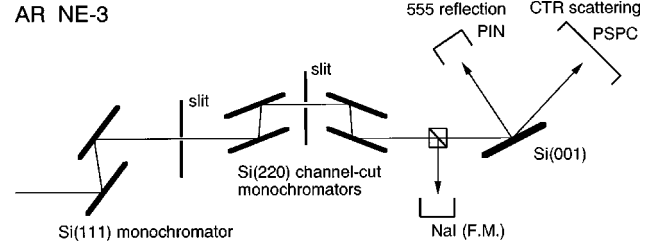


FIG. 5. Experimental arrangement used to study influence of Bragg scattering on CTR scattering.

#### IV. EXPERIMENTAL RESULT

Figure 5 shows the experimental arrangement to confirm the prediction given in the previous two sections. The experiment was done at the experimental station of the beamline AR-NE3 in KEK, where a high brilliance x-ray beam is available from an in-vacuum undulator installed in the Accumulation Ring.<sup>24</sup> A single crystalline Si(001) (60 mm  $\times$  40 mm  $\times$  10.5 mm) was used as a sample. We measured the intensity of CTR scattering along the 00 rod under exciting the 555 Bragg reflection as shown in Fig. 6.

The  $\sigma$  polarized beam, premonochromatized by a Si(111) double-crystal monochromator, was more highly monochromatized by two Si(220) channel-cut crystals arranged in the (+ +) geometry. The value of  $\Delta\lambda/\lambda$  is of the order of  $10^{-6}$ . This monochromatization is required to obtain modulation profiles without suffering the smearing effect due to dispersion of wavelength. As a result, the number of photons that could reach the sample was about  $10^7$  cps, which is too weak to perform measurements sensitive to the surface structure. Thus we measured intensities of CTR scattering along the 00 rod relatively close to the 004 Bragg point, where the reflectivity of CTR scattering is of the order of  $10^{-7}$  but the intensity profile is not so sensitive to the surface structure, as is expected from Fig. 3(a). The value of  $l$  for the 00 rod was about 3.946. The wavelength of x rays was fixed at 1.24053 Å, which was experimentally determined by the difference between the incident angles giving 004 and 555 Bragg reflections.

The beam intensity impinging on the sample was monitored by an NaI scintillation counter placed before the sample, and the signal was normalized by its counts. The intensities of 555 Bragg reflection and 00 rod CTR scattering

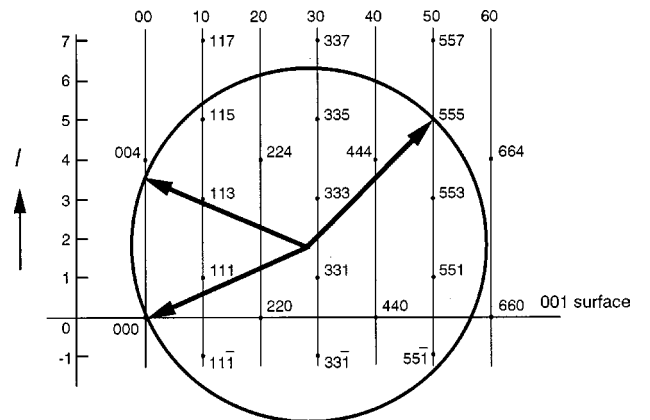


FIG. 6. Geometry used in the experiment.

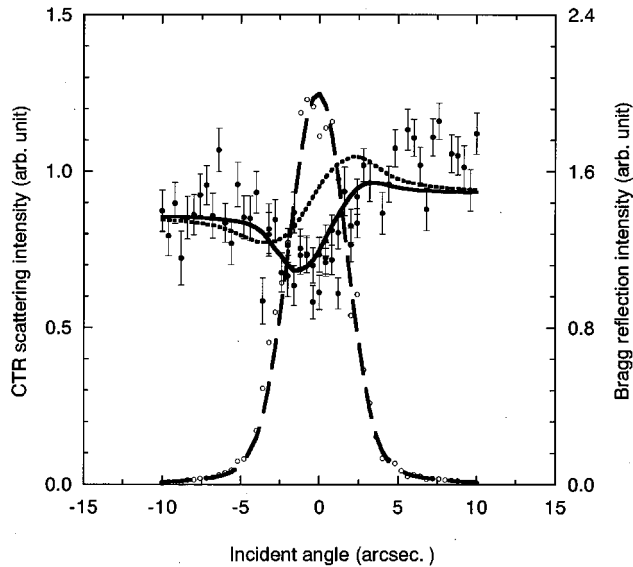


FIG. 7. Experimental results on 555 Bragg reflection and CTR scattering along the 00 rod. Open and filled circles show the intensities of 555 reflection and 00 rod CTR scattering, respectively. Broken and dotted lines represent the intensities of 555 Bragg reflection and 00 rod CTR scattering calculated for a perfect crystal by the dynamical theory. Solid line was calculated for a model in which surface layers of the silicon crystal are distorted by the native oxide layer.

were detected by a PIN photodiode and a PSPC (position sensitive proportional counter), respectively. Spot intensities observed by the PSPC were integrated after subtraction of the background. A typical intensity for the 00 rod was about a few cps.

The result is shown in Fig. 7, where open and filled circles mean the intensities of 555 reflection and 00 rod CTR scattering, respectively. The broken and dotted lines represent the intensities of 555 Bragg reflection and 00 rod CTR scattering calculated for a perfect crystal by the dynamical theory given in Sec. II. It is clearly seen that the CTR scattering intensity is indeed modulated by the Bragg reflection. However, there is a slight difference between the observed curve of the CTR scattering and the curve calculated for an ideally truncated Si single crystal indicated by the dotted line. This difference will be discussed in the following section.

## V. DISCUSSION

First, we discuss the slight difference seen in Fig. 7. The experiment was done in the atmosphere. Thus a native oxide layer about a few tens of Å in thickness is formed on the substrate silicon crystal. But it is obvious that neither the scattering from the native oxide layer nor that from the local structure at the interface between the native oxide layer and the silicon crystal can explain the difference because the CTR scattering was measured at a point close to the Bragg point, as is understood from Fig. 3(a). However there is a possibility that the native oxide layer brings about strain fields spreading into the substrate crystal.

One can show that such strain changes only the phase of

the CTR scattering and does not change the intensity of Bragg reflection if the range of the strain field is sufficiently larger than the lattice spacing and small enough compared to the extinction depth of the Bragg reflection, and the accumulated total shift at the top layer of the substrate silicon crystal from the ideally truncated position is small compared to the lattice spacing.

Simulations showed that the phase of the CTR scattering is most sensitive to the total shift of the lattice plane at the top of the silicon crystal. Thus, we obtained the total shift by the least-squares fits assuming a simple model in which  $N$  layers of the silicon crystal surface have a constant lattice distortion of  $\Delta d/d$ . The best fits were obtained at  $-0.15$  Å for the total shift when  $N=228$ , corresponding to the depth of 310 Å, and  $\Delta d/d=-0.0005$ . The result is shown as the solid line in Fig. 7. The value of  $\chi^2$  was improved to be 1.9 from 3.3.

Recently, this kind of strain field, which may depend on the macroscopic shape of the sample and the structure of the oxide layer, has been observed by using extremely asymmetric x-ray diffraction.<sup>25</sup> It is noteworthy that the present method has a potential to be used for investigating such strain field near the surface.

Next, we discuss the features of the present method. We showed that the method presented in the work has a similarity with the x-ray standing-wave method. In the conventional standing-wave method, the yield of secondary emission such as fluorescence is observed in proportion to the field intensity at emission atoms in surface sensitive measurements. In a similar sense, when x-ray scattering amplitude by a surface layer is larger than CTR scattering amplitude by the substrate, x-ray intensity elastically scattered by the system reflects the intensity of the standing-wave field formed by Bragg reflection at the surface layer. Therefore, in the case of measurements of fractional-order rods, not including x-ray scattering from the substrate, the profile of intensity changes become quite sensitive to the surface structure. This is the case even for reconstructed surfaces formed by the same atoms as the substrate, in contrast to XSW. Another difference of the method from XSW is that the profile of the intensity curve for a 100% displacement of diffracting plane is not identical to that for no displacement (0%) as is understood from Eq. (2).

In the present method, the intensity of CTR scattering depends not only on the incident beam but also on the Bragg reflected beam by the effect of *Umweganregung*, so that the profile of the intensity change is sensitive to two-dimensional structure on the scattering plane in the coplanar case. Therefore, in principle, the profile of the intensity change in noncoplanar geometry has three-dimensional information on the surface structure. This indicates that the method presented here has a possibility of determining the three-dimensional surface structure by scanning only a small angular range, which has an advantage when the sample is not so uniform and has the surface structure on a restricted area.

## VI. CONCLUSION

Effects of Bragg reflection on CTR scattering are calculated based on Darwin's dynamical theory extended to a

three-beam case. The results showed the profile of the intensity change of CTR scattering is sensitive to surface structures. It was found that the kinematical calculation reproduces the dynamical one quite well if the intensity of CTR scattering is sufficiently weak compared with the Bragg intensity, which is usually the case. It was also shown by kinematical treatment that the intensity of CTR scattering shows a similar change as that of the standing-wave field at the surface layer when the amplitude of x-ray scattering by the surface layer is large compared with the CTR scattering amplitude by the substrate. A preliminary experimental result obtained for a Si(001) crystal agrees with the theoretical one although the experiment was done at the condition not so sensitive to the surface structure. Further analysis improves the fitting between the two if we assume that the strain field caused by the native oxide layer extends from the top of the silicon crystal into the depth of a few hundreds of Å.

#### ACKNOWLEDGMENTS

The authors would like to thank S. Nakatani and Y. Ito for discussions and Y. Yoda for providing them with channel-

cut crystals. The present work was partly supported by a Grant-in-Aid for Scientific Research (Nos. 09304035 and 09440151) from the Ministry of Education, Science, Sports, and Culture.

#### APPENDIX

In this appendix, we treat a perfect crystal of semi-infinite thickness. In Darwin's dynamical theory, the crystal is divided into atomic layers parallel to the crystal surface. The atomic layer corresponds to a unit cell defined parallel to the surface. Thus the definition of the unit cell does not always coincide with that in the conventional 3D crystallography, and is rather consistent with that in the kinematical theory of surface diffraction.<sup>1</sup>

First, we consider a perfect crystal of finite thickness. Intensities diffracted by an ideal crystal of  $N+1$  layers,  $R_{H_1, N+1}$  and  $R_{H_2, N+1}$ , have a relation with those of  $N$  layers,  $R_{H_1, N}$  and  $R_{H_2, N}$ , in the Bragg-case of three-beam coplanar geometry.<sup>10</sup>

$$R_{H_1, N+1} = \frac{r_{H_1} + (t_0 t_{H_1} - r_{H_1} r_{\overline{H_1}}) \Phi_0 \Phi_{H_1} R_{H_1, N} + (t_0 r_{H_1 - H_2} - r_{H_1} r_{\overline{H_2}}) \Phi_0 \Phi_{H_2} R_{H_2, N}}{1 - (r_{\overline{H_1}} \Phi_0 \Phi_{H_1} R_{H_1, N} + r_{\overline{H_2}} \Phi_0 \Phi_{H_2} R_{H_2, N})}, \quad (\text{A1})$$

$$R_{H_2, N+1} = \frac{r_{H_2} + (t_0 r_{H_2 - H_1} - r_{\overline{H_1}} r_{H_2}) \Phi_0 \Phi_{H_1} R_{H_1, N} + (t_0 t_{H_2} - r_{H_2} r_{\overline{H_2}}) \Phi_0 \Phi_{H_2} R_{H_2, N}}{1 - (r_{\overline{H_1}} \Phi_0 \Phi_{H_1} R_{H_1, N} + r_{\overline{H_2}} \Phi_0 \Phi_{H_2} R_{H_2, N})}, \quad (\text{A2})$$

where  $r$ 's are  $t$ 's are reflection and transmission coefficients of a layer calculated by Fresnel's diffraction theory and related to the structure factors for the layer.<sup>10,23</sup> For instance,  $r_{H_1}$  is given by

$$r_{H_1} = i \frac{C \lambda r_e}{|\cos \Theta_{H_1}|} \frac{F_{H_1}}{S}, \quad (\text{A3})$$

where  $r_e$  is the classical radius of an electron,  $S$  is the area of the unit cell, and  $F_{H_1}$  is the structure factor for the surface layer. Phase factors  $\Phi_0$ ,  $\Phi_{H_1}$ , and  $\Phi_{H_2}$  are defined by

$$\begin{aligned} \Phi_0 &= \exp\left(-i2\pi \frac{d \cos \Theta_0}{\lambda}\right), \\ \Phi_{H_1} &= \exp\left(-i2\pi \frac{-d \cos \Theta_{H_1}}{\lambda}\right), \\ \Phi_{H_2} &= \exp\left(-i2\pi \frac{-d \cos \Theta_{H_2}}{\lambda}\right), \end{aligned} \quad (\text{A4})$$

where  $\Theta_0$ ,  $\Theta_{H_1}$ , and  $\Theta_{H_2}$  are incident and scattered angles measured from the inward surface normal as depicted in Fig. 1(a), and asymmetric factors for the two reflections are given by  $b_{H_1} = \cos \Theta_0 / \cos \Theta_{H_1}$  for  $H_1$  reflection, and  $b_{H_2}$

$= \cos \Theta_0 / \cos \Theta_{H_2}$  for  $H_2$  reflection,  $d$  being the distance between the layers constituting the crystal.

Diffracted intensities by an ideal perfect crystal of semi-infinite thickness,  $R_{H_1}^B$  and  $R_{H_2}^B$  may be calculated from the coupled equations (A1) and (A2) by putting  $R_{H_2, N+1} = R_{H_2, N} = R_{H_2}^B$  and  $R_{H_1, N+1} = R_{H_1, N} = R_{H_1}^B$ . Then the coupled equations are reduced to a cubic equation of  $R_{H_1}^B$  or  $R_{H_2}^B$ . For instance, the cubic equation for  $R_{H_2}^B$  is expressed as

$$a_1 R_{H_2}^B{}^3 + a_2 R_{H_2}^B{}^2 + a_3 R_{H_2}^B + a_4 = 0, \quad (\text{A5})$$

where

$$a_1 = b^2 c P r_{\overline{H_1}}{}^2 + b c r_{\overline{H_2}} r_{\overline{H_1}} (cM - bL) - b c^2 Q r_{\overline{H_2}}{}^2, \quad (\text{A6})$$

$$\begin{aligned} a_2 &= b(cM - bL) \{ r_{\overline{H_1}} (cM - 1) + c Q r_{\overline{H_2}} \} \\ &\quad + b r_{\overline{H_1}} (c r_{H_2} r_{\overline{H_2}} + b r_{H_1} r_{\overline{H_1}} + 2bcPQ) \\ &\quad - 2bcQ(cM - 1) r_{\overline{H_2}}, \end{aligned} \quad (\text{A7})$$

$$\begin{aligned} a_3 &= b r_{H_2} r_{\overline{H_1}} (cM - bL) + b(cM - 1) \{ r_{H_2} r_{\overline{H_1}} - Q(bL - 1) \} \\ &\quad + bQ(2b r_{H_1} r_{\overline{H_1}} - c r_{H_2} r_{\overline{H_2}} + bcPQ), \end{aligned} \quad (\text{A8})$$

$$a_4 = br_{H_2}^2 r_{\overline{H}_1} + b^2 Q^2 r_{H_1} - bQr_{H_2}(bL - 1) \quad (\text{A9})$$

with the definitions of

$$L = t_0 t_{H_1} - r_{H_1} r_{\overline{H}_1}, \quad (\text{A10})$$

$$M = t_0 t_{H_2} - r_{H_2} r_{\overline{H}_2}, \quad (\text{A11})$$

$$P = t_0 r_{H_1 - H_2} - r_{\overline{H}_2} r_{H_1}, \quad (\text{A12})$$

$$Q = t_0 r_{H_2 - H_1} - r_{H_2} r_{\overline{H}_1}, \quad (\text{A13})$$

and

$$b = \Phi_0 \Phi_{H_1}, \quad (\text{A14})$$

$$c = \Phi_0 \Phi_{H_2}. \quad (\text{A15})$$

Once  $R_{H_2}^B$  is obtained,  $R_{H_1}^B$  is calculated by

$$R_{H_1}^B = - \frac{(A_1 R_{H_2}^B)^2 + B_1 R_{H_2}^B + r_{H_2}}{(C_1 R_{H_2} + D_1)}, \quad (\text{A16})$$

where

$$A_1 = cr_{\overline{H}_2}, \quad (\text{A17})$$

$$B_1 = cM - 1, \quad (\text{A18})$$

$$C_1 = br_{\overline{H}_1}, \quad (\text{A19})$$

$$D_1 = bQ. \quad (\text{A20})$$

\*Author to whom correspondence should be addressed. Electronic address: ttaka@issp.u-tokyo.ac.jp

<sup>†</sup>Present address: SPring-8/JAERI, 323-3, Mihara Mikazuki-chou, Sayo-gun, Hyogo 679-5143, Japan.

<sup>1</sup>I.K. Robinson, *Handbook on Synchrotron Radiation*, edited by G. Brown and D.E. Moncton (Elsevier, New York, 1991), Vol. 3, Chap. 7.

<sup>2</sup>R. Feidenhans'l, *Surf. Sci. Rep.* **10**, 105 (1989).

<sup>3</sup>P. Eisenberger and W.C. Marra, *Phys. Rev. Lett.* **46**, 1081 (1981).

<sup>4</sup>I.K. Robinson, *Phys. Rev. B* **33**, 3830 (1986).

<sup>5</sup>R. Feidenhans'l, M. Nielsen, F. Grey, R.L. Johnson, and I.K. Robinson, *Surf. Sci.* **186**, 499 (1986).

<sup>6</sup>T. Takahashi, S. Nakatani, T. Ishikawa, and S. Kikuta, *Surf. Sci.* **191**, L825 (1987).

<sup>7</sup>I.K. Robinson, *Phys. Rev. B* **35**, 3910 (1987).

<sup>8</sup>I.K. Robinson, R.T. Tung, and R. Feidenhans'l, *Phys. Rev. B* **38**, 3632 (1988).

<sup>9</sup>S.G.J. Mochrie, D.M. Zehner, B.M. Ocko, and D. Gibbs, *Phys. Rev. Lett.* **64**, 2925 (1990).

<sup>10</sup>T. Takahashi and S. Nakatani, *Surf. Sci.* **326**, 347 (1995).

<sup>11</sup>B.W. Batterman and H. Cole, *Rev. Mod. Phys.* **36**, 681 (1964).

<sup>12</sup>R. Colella, *Phys. Rev. B* **43**, 13 827 (1991).

<sup>13</sup>A. Caticha, *Phys. Rev. B* **47**, 76 (1993).

<sup>14</sup>A. Caticha, *Phys. Rev. B* **49**, 33 (1994).

<sup>15</sup>S. Nakatani and T. Takahashi, *Surf. Sci.* **311**, 433 (1994).

<sup>16</sup>T.-S. Gau and S.-L. Chang, *Acta Crystallogr., Sect. A: Found. Crystallogr.* **51**, 920 (1995).

<sup>17</sup>T.-S. Gau, H.-C. Chien, S.-L. Chang, M.-Y. Li, and M.-K. Wu, *Surf. Sci.* **384**, 254 (1997).

<sup>18</sup>T. Takahashi, *J. Phys. Soc. Jpn.* **65**, Suppl. A, 271 (1996).

<sup>19</sup>R. Colella, *Acta Crystallogr., Sect. A: Cryst. Phys., Diffraction, Theor. Gen. Crystallogr.* **A30**, 413 (1974).

<sup>20</sup>S.-L. Chang, *Multiple Diffraction of X-rays in Crystals* (Springer, Berlin, 1984).

<sup>21</sup>O. Litzman, P. Mikulik, and P. Dub, *J. Phys.: Condens. Matter* **8**, 4709 (1996).

<sup>22</sup>C.G. Darwin, *Philos. Mag.* **27**, 675 (1914).

<sup>23</sup>B.E. Warren, *X-ray Diffraction* (Addison-Wesley, Reading, MA, 1969).

<sup>24</sup>X. Zhang, T. Mochizuki, H. Sugiyama, S. Yamamoto, H. Kitamura, T. Sioya, M. Ando, Y. Yoda, T. Ishikawa, S. Kikuta, and C.K. Suzuki, *Rev. Sci. Instrum.* **63**, 404 (1992).

<sup>25</sup>T. Emoto, K. Akimoto, and A. Ichimiya, *Surf. Sci.* **438**, 107 (1999).